Identification and Characterization of an Escorter for Two Secretory Adhesins in *Toxoplasma gondii*

Matthias Reiss,* Nicola Viebig,* Susan Brecht,* Marie-Noelle Fourmaux,‡ Martine Soete,‡ Manlio Di Cristina,§ Jean François Dubremetz,‡ and Dominique Soldati*

*Center for Molecular Biology, University of Heidelberg, Heidelberg D-63120, Germany; ‡Institute of Biology CNRS, Institut Pasteur de Lille, Lille, 59019 France; and §Department of Cell Biology, Imperial College of Science, Technology, and Medicine, London, SW7 2AZ United Kingdom

Abstract. The intracellular protozoan parasite *Toxoplasma gondii* shares with other members of the Apicomplexa a common set of apical structures involved in host cell invasion. Micronemes are apical secretory organelles releasing their contents upon contact with host cells. We have identified a transmembrane micronemal protein MIC6, which functions as an escorter for the accurate targeting of two soluble proteins MIC1 and MIC4 to the micronemes. Disruption of *MIC1*, *MIC4*, and *MIC6* genes allowed us to precisely dissect their contribution in sorting processes. We have mapped domains on these proteins that determine complex formation and targeting to the organelle. MIC6 carries a sorting signal(s) in its cytoplasmic tail whereas its association with MIC1 involves a lumenal EGF-like domain. MIC4 binds directly to MIC1 and behaves as a passive cargo molecule. In contrast, MIC1 is linked to a quality control system and is absolutely required for the complex to leave the early compartments of the secretory pathway. MIC1 and MIC4 bind to host cells, and the existence of such a complex provides a plausible mechanism explaining how soluble adhesins act. We hypothesize that during invasion, MIC6 along with adhesins establishes a bridge between the host cell and the parasite.

Key words: parasite • *Toxoplasma gondii* • protein targeting • regulated secretion • EGF-like domain

Introduction

The first and essential event in obligate intracellular parasite infection is host cell invasion. In apicomplexan parasites, apical secretory organelles ensure the accumulation and the appropriate release in time and space of adhesins and other invasion factors. An increasing number of micronemal proteins sharing common features have been identified among the Apicomplexa and recent studies illustrated their central role in parasite motility and host cells invasion (for review see Tomley and Soldati, 2001). *Toxoplasma gondii* has developed a remarkable ability to actively penetrate a broad range of cells within the mammalian hosts, whereas the members of the *Plasmodium* genus exhibit very restricted host range specificities. The molecular bases of host range specificity have not been elucidated yet but might implicate the repertoire of micronemal proteins and their adhesive interactions with host cell receptors (Barnwell and Galinski, 1995). The micronemal proteins of the TRAP family have been identified as active players in host cell invasion and gliding motility in the invasive stages of the rodent malaria parasites *Plasmodium berghei* (Sultan et al., 1997; Dessens et al., 1999; Yuda et al., 1999). Thrombospondin-related adhesive proteins (TRAPs) contain a putative transmembrane spanning domain and a conserved short cytoplasmic tail. MIC2, the homologue of TRAP in *T. gondii* (Wan et al., 1997), is shed apically on the surface of the parasites and relocalizes toward the posterior pole by a mechanism dependent on the parasite actomyosin system (Sibley et al., 1998). In a recent complementation experiment, the cytoplasmic domain (CD)[1] of MIC2 was shown to functionally replace the corresponding domain in PbTRAP (Kappe et al., 1999), suggesting that the machinery for invasion is conserved among members of the phylum. We have identified a novel family of transmembrane micronemal proteins including MIC6 (Meissner, M., and D. Soldati, unpublished results; sequence data are available from GenBank/EMBL/DDBJ under accession number AF110270). Analysis of the de-

M. Reiss and N. Viebig contributed equally to this study.

Address correspondence to D. Soldati, ZMBH, Im Neunheimer Feld 282, P.O. Box 106249, Heidelberg D-69120, Germany. Tel.: 49-6221-54-68-70. Fax: 49-6221-54-58-92. E-mail: soldati@zmbh.uni-heidelberg.de

[1]*Abbreviations used in this paper:* CD, cytoplasmic domain; GPI, glycosylphosphatidyl-inositol; HFF, human foreskin fibroblast; IFA, indirect immunofluorescence assay; PBSFCS, 10% PBS FCS; RH, wild-type parasite of RH strain; TM-CD^{MIC6}, transmembrane and CD of the MIC6; TRAP, thrombospondin-related adhesive protein.

duced amino acid sequence of MIC6 revealed a secretory signal sequence and three EGF–like domains. The COOH-terminal region exhibits a putative transmembrane spanning domain and a short cytoplasmic tail homologous to MIC2 and to the other members of the TRAP family. Four soluble micronemal proteins, MIC1, MIC3, MIC4, and MIC5 have been characterized so far in *T. gondii*. These proteins contain multiple thrombospondin-like, EGF-like, or apple domains potentially conferring adhesive properties to these molecules (see Fig. 1 A). Indeed, MIC1 (Fourmaux et al., 1996), MIC3 (Garcia-Réguet et al., 2001), and MIC4 (Brecht et al., 2001) bind to host cells, but it is still unclear how they establish a link between the parasite and the host cell. Similarly, little is known about how in general soluble secretory proteins are sorted to their appropriate organelles. Understanding how *T. gondii* copes with the sorting of the large variety of secreted proteins in the multiple distinct secretory compartments is an area of intense investigation (Kaasch and Joiner, 2000; Ngo et al., 2000). Recent studies have demonstrated that the targeting of transmembrane proteins in specialized organelles is achieved through the use of evolutionary conserved signals and machinery (Hoppe et al., 2000).

In this study, we have abrogated the expression of MIC1, MIC4, or MIC6 by gene disruption. Analysis of these mutants demonstrated that the sorting of the two soluble proteins MIC1 and MIC4 to micronemes is critically dependent on the presence of the transmembrane protein MIC6. We confirmed the existence of a complex between these three micronemal proteins and mapped some of the domains involved in protein–protein interactions and sorting. Such a complex potentially explains how soluble secretory adhesins can be sorted, and how they could contribute efficiently to the invasion process.

Materials and Methods

Host Cells and Toxoplasma Strains Growth

Tachyzoites of the wild-type parasite of RH strain (RH) *T. gondii* were maintained by growth on monolayers of human foreskin fibroblasts (HFF) or on African green monkey (Vero) cells, grown in DME (GIBCO) containing 5 or 10% fetal calf serum (GIBCO). A clonal isolate of the RHhxgprt of *T. gondii,* was used as the recipient strain for the experiments described here.

DNA Constructs

The vectors for the replacement of *MIC1*, *MIC4*, and *MIC6* genes were generated by insertion of large 5′ and 3′ flanking sequences of the MIC genes in the vector pdhfrtsHXGPRT to give pmic1koHXGPRT, pmic4koHXGPRT, and pmic6koHXGPRT, respectively. Approximately 2,500 bp of 5′ and 3,000 bp of 3′ flanking sequences of *MIC1* gene, 1,561 bp of 5′ and 1,726 bp of 3′ flanking sequences of *MIC4* gene and 1,788 kb of 5′, and 2,257 kb of 3′ flanking sequences of *MIC6* gene were used.

Construction of mic6 Mutants

All MIC4 and MIC6 mutants were cloned in pT (pT/5R230), a plasmid derived from pBluescript II SK$^+$ (Stratagene) containing the promoter sequence of the *TUB1* gene, a 3′ untranslated sequence (3′UTR) of *SAG1*, described previously (Soldati and Boothroyd, 1995). MIC1 and SAG1 mutants were cloned into pM2 vector, which contains 1,479 bp of 5′ and 1,200 bp of 3′ flanking sequence of the *MIC2* gene as recently described (Di Cristina et al., 2000).

The pTMIC6 construct was obtained by PCR amplification of the full MIC6 cDNA using primers MIC6/5 and MIC6/6 and cloning into EcoRI and PacI sites of pT/5R230. The Ty-1 epitope tag, EVHTNQDPLDG, previously described (Bastin et al., 1996) was introduced by inverse PCR at the amino acid position 195. One of the primers contains the sequence corresponding to the tag and both primers contain a unique restriction site not present on the vector (NsiI) and matching sequence in sense and antisense direction at the site of tag insertion. The whole plasmid was amplified by inverse PCR, cut with NsiI, and ligated. The amplified plasmid was then cut with NsiI and ligated. The XbaI restriction site was introduced during amplification using the primers Ty-1/1 and Ty-1/2 to generate pTMIC6Ty-1. The construct pTMIC6ΔCD was obtained by PCR amplification of MIC6 lacking the last 31 amino acids and deletion of the tyrosine residue 311, using the primers MIC6/5 and MIC6/7. The construct pTMIC6GPI was cloned in two steps. The fragment encoding the glycosylphosphatidyl-inositol (GPI) signal from SAG1 was amplified by PCR and cloned between the NsiI and PacI sites in pT/5R230 to generate pTGPI using the primers SAG1/1 and T3. Subsequently, the MIC6 NH_2-terminal domain was amplified by PCR using the primers MIC6/5 and MIC6/8 and cloned into pTGPI between EcoRI and NsiI sites. The construct pTMIC6TyGPI was obtained by the amplification of MIC6Ty from pTMIC6Ty and insertion into pTGPI as described above. MIC6 mutants lacking an EGF-like domain were generated by inverse PCR creating a new NsiI introduced in the primers. The constructs pTMIC6ΔEGF-1, pTMIC6ΔEGF-2, and pTMIC6ΔEGF-3 were generated by combining primers MIC6/9 with MIC6/17, MIC6/9 with MIC6/16, and MIC6/11 with MIC6/12, respectively. Inverse PCR was also used to generate pTMIC6ΔAD, using primers MIC6/13 and MIC6/14. The construct pM2SAG1TM-CD was obtained by exchanging the CD of MIC2 by the CD of MIC6 in the construct pSAG1/TM-CD^{MIC2} (Di Cristina et al., 2000). This vector expresses SAG1 under the control of the 5′ and 3′ flanking sequences of *MIC2*. The GPI anchoring signal of SAG1 has been replaced by the transmembrane and CD of MIC6 (TM-CD^{MIC6}) obtained by PCR amplification using the primers MIC6/15 and MIC6/6 and cloned into SalI and PacI sites. A Ty-1 epitope tag was introduced by insertion of double-stranded oligonucleotides into the SalI site using the primers Ty-1/5 and Ty-1/6.

Construction of mic4 Mutants

The pTMIC4 construct was obtained by PCR amplification of the full-length MIC4 cDNA using primers MIC4/1 and MIC4/2 and cloning into EcoRI and PacI sites of pT/5R230. The vector pTMIC4Ty-1 was generated by the insertion of annealed oligonucleotides Ty-1/3 and Ty-1/4 into the unique PstI site of *MIC4* cDNA at amino acid position 46. Apple domains deletion mutants of MIC4 were obtained by PCR amplification to generate truncated cDNA and cloning into pT/5R230. Primers MIC4/1 and MIC4/3 were used to generate pTMIC4ΔA5-6 and primers MIC4/1 and MIC4/4 for pTMIC4ΔA3-6. All PCR amplifications were carried out using *Pfu* DNA polymerase, which exhibits the lowest error rate of any thermostable DNA polymerase. The PCR reactions were performed in a total volume reaction of 50 μl for 25 cycles of 96°C (1 min), 55–60°C (1 min), and 72°C (1.5 min) using a thermal cycler. All constructs were sequenced. The cDNA of MIC1 was obtained by RT-PCR amplification and cloned into the vector pM2myc to generate pM2MIC1myc.

The following primers were used: Ty-1/1, 5′-CCTCTAGACCCCCATTATAGGAAGCCTCCC-3′; Ty-1/2, 5′-CGTCTAGAGGATCCTGGTTAGTGTGCACCTCAGGCACACGCTTGCAGGT-3′; Ty-1/3, 5′-GAGGTCCACACGAACCAGGACCCGCTCGACCATGCA-3′; Ty-1/4, 5′-TGGTCGAGCGGGTCCTGGTTCGTGTGGACCTCTGCA-3′; Ty-1/5, 5′-TCGAGCGTCCACACCAACCAGGACCCCCTCGACGGG-3′; Ty-1/6, 5′-TCGACGTCGAGGGGGTCCTGGTTGGTGTGGACC-3′; MIC6/1, 5′-GGGGTACCCTGTGGCGACGGGACCAT-3′; MIC6/2, 5′-GGGGTACCATGCATAGCAGAGACGCGCGGC-3′; MIC6/3, 5′-CGGGATCCTTAATTAACACGTTCTCGGCTGAGACTTCA-3′; MIC6/4, 5′-GTGGGGGAACCGTGGATCC-3′. MIC6/5, 5′-CGGAATTCCCTTTTTCGACAAAATGAGGCTCTTCCGGTGCTG-3′; MIC6/7, 5′-CCTTAATTAACCGGATCCCTTTCTCATTGCAACACCCGCTCC-3′; MIC6/8, 5′-CGGGATCCATGCATGTCCACTTCCTTCCTCT-3′; MIC6/9, 5′-CCTTAATTAAGATGCATTGTCTGCAATCTCTCCATTCC-3′; MIC6/10, 5′-CCAATGCATCTGTAAGACAGGAAAGCGGCTG-3′; MIC6/11, 5′-CCAATGCATGCAAGCGTGTGCCTGAGGTG-3′; MIC6/12, 5′-TGGATGCATTGCCGCTTTCCTGTCTTACAAT-3′; MIC6/13, 5′-CCTTAATTAAGATGCATGGGGGTCTAGAGGATCCTG-3′; MIC6/14, 5′-CCAATGCATTAGGAAGTGGACATGCTGGTGCG-3′; MIC6/15, 5′-GGGCCCGTCGACGAAGGAAGTGGACATGCTGG-3′; MIC6/16, 5′-TGGATGCATTAGCCATGGGTACACCTGAGG-3′; MIC6/17, 5′-CCAATGCATCAGGTGTACCCATGGCTAATT-3′; MIC4/1, 5′-CGGAATTCCCTTTTTCGACAAAATGAGAGCGTCGCTCCC-3′; MIC4/2, 5′-CCTTAATTAAAATGCATCTTCTGT-

GTCTTTCGCTTC-3′; MIC4/3, 5′-CCTTAATTAATCAGGATCCGCCA-AAATCGCAGAACTCC-3′; and MIC4/4, 5′-CCTTAATTAAGATGCA-TCTTCCATCTCCTCTTGAGTTAA-3′.

Transfection and Selections

Disruptions of *MIC1*, *MIC4*, and *MIC6* genes were obtained by double homologous recombination using Tg*HXGPRT* as selectable marker into the RHhxgprt$^-$ background. The complementation of mic1ko, mic4ko, and mic6ko were achieved by cotransfection with a selectable plasmid expressing the chloramphenicol acetyltransferase (CAT) gene as previously described (Soldati and Boothroyd, 1993).

To generate stable transformants, 5×10^7 extracellular RHhxgprt$^-$ parasites were transfected and selected as previously described (Donald et al., 1996), with the modifications described below. Parasites were transfected with 80–100 μg of linearized plasmid. 24 h later, parasites were subjected to mycophenolic acid/Xanthine (MPA/X) exposure and cloned 3–5 d later by limiting dilution in 96-well microtiter plates containing HFF cells in the presence of MPA/X. To generate *MICs* knockout recombinants, four transfections using 10^8 freshly released parasites with 25, 50, 75, or 100 μg of linearized plasmid were conducted in parallel. Pools of stable transformants were analyzed by indirect immunofluorescence assay (IFA) for the absence of MIC1, MIC4, or MIC6 protein, respectively. Selection for the presence of *HXGPRT* marker gene was achieved as described above, whereas selection for the presence of CAT was done as previously described (Kim et al., 1993). Stable transformants obtained under chloramphenicol selection were cloned by limiting dilution 6 d after the beginning of chloramphenicol treatment.

SDS-PAGE and Immunoblots

SDS-PAGE was performed according to Laemmli (1970). Freshly released tachyzoites were harvested, washed in PBS, and lysed in RIPA solution (150 mM NaCl, 1% Triton X-100, 0.5% deoxycholate, 0.1% SDS, 50 mM Tris, pH 8.0, 1 mM EDTA). Polyacrylamide gels (8.5–10%) were run under reducing condition with 0.1 M dithiotreitol in samples. mAbs (mouse ascitic fluid) and rabbit polyclonal antisera were diluted 1:1,000 in PBS, 0.05% Tween 20, and 5% nonfat milk powder. After washing, the nitrocellulose membrane was incubated for 1 h with a peroxidase-conjugated goat anti–mouse antibody (Bio-Rad Laboratories) and bound antibodies visualized using the ECL system, POD (Boehringer).

Immunoprecipitation

Freshly lysed parasites (5×10^9) were washed and resuspended into 2-ml PBS in presence of a mix protease inhibitors (complete protease inhibitor mix; Roche) and sonicated for 1 min (30% pulse small tip 6; Branson Sonifier). Cell rupture was checked under the microscope and followed by centrifugation for 30 min at 45,000 rpm, using a TL45 rotor in a Beckman Coulter ultracentrifuge. The supernatant was then incubated with antibodies overnight at 4°C under agitation. Lysates incubated in absence of antibodies and antibodies incubated in absence of lysate were included as controls. 200 μl of 10% Sepharose A CL4B slurry in PBS was added to each sample and incubated again for 1 h at 4°C under agitation. The beads were washed four times in 1 ml PBS, and 50 μl of sample buffer with 0.1 M DTT was added before boiling and loading on SDS-PAGE.

Indirect Immunofluorescence Microscopy

All manipulations were carried out at room temperature. Tachyzoites-infected HFF cells on glass coverslips were fixed with 3% paraformaldehyde, 0.05% glutaraldehyde, or 4% paraformaldehyde only for 20 min, followed by 3-min incubation with 0.1 M glycine in PBS. Fixed cells were permeabilized with 0.2% Triton X-100 in PBS for 20 min and blocked in 2% FCS or BSA in PBS for 20 min. The cells were then stained with the primary antibodies followed by Alexa 594 goat anti–rabbit or Alexa 488–conjugated goat anti–mouse antibodies (Molecular Probes; Cappel; and Bio-Rad Laboratories). Confocal images were collected with a Leica laser scanning confocal microscope (TCS-NT DM/IRB) using a 100× Plan-Apo objective with NA 1.30. Single optical sections were recorded with an opti-

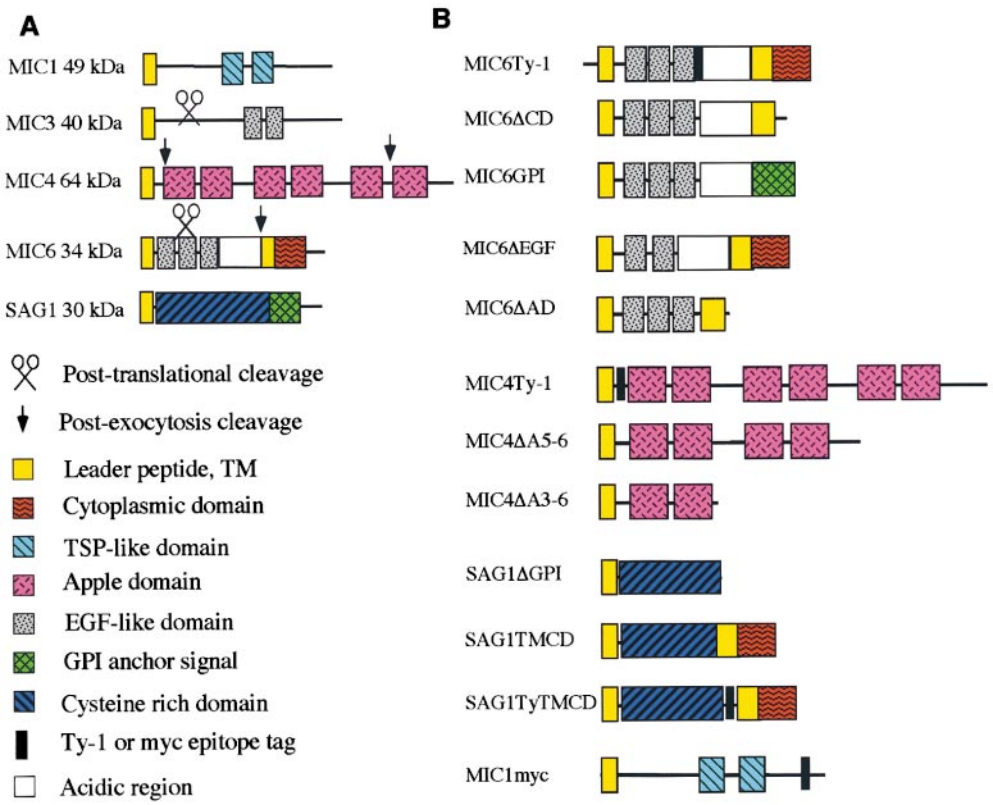

Figure 1. Illustration of the structural domains of the proteins and the recombinant mutants used in this study. (A) Schematic representation of the structural domains on the micronemal proteins MIC1, MIC3, MIC4, MIC6, and the major tachyzoite surface antigen SAG1. The proteolytic cleavages of the micronemal proteins are indicated with two types of symbols distinguishing posttranslational and postexocytosis cleavages. Sequence data for MIC1, MIC4, and MIC6 are available from GenBank/EMBL/DDBJ under accession numbers Z71786, AF143487, and AF110270, respectively. (B) Schematic representation of the constructs used in this study. The epitope tags Ty-1 and myc are represented by a black box. The color code of the diverse domains is as described in A. Schematic drawing of pTMIC6Ty-1, pTMIC6ΔCD, pTMIC6GPI, pTMIC6ΔEGF-1, -2, or -3, pTMIC6ΔAD, pTMIC4Ty-1, pTMIC4ΔA5-6, pTMIC4ΔA3-6, pM2SAG1TM-CD, and pM2MIC1myc.

mal pinhole of 1.0 (according to Leica instructions) and 16 times averaging. Other micrographs were obtained with a Zeiss Axiophot equipped with a charge-coupled device camera (CH-250; Photometrics). Adobe® Photoshop™ was used for image processing.

Immunoelectron Microscopy

Infected monolayers were fixed by mixing the culture medium with one volume of 4% paraformaldehyde minus 0.2% glutaraldehyde in 0.2 M sodium phosphate buffer, pH 7.5, and incubating for 15 min at room temperature, followed by doubling the total volume by addition of culture medium and incubating for 90 min. The fixed infected cells were then washed in 10% PBS FCS (PBSFCS), scraped with a teflon blade, and infused in 2.3 M sucrose containing 10% polyvinylpyrrolidone before being frozen in liquid nitrogen. Sections were obtained on a Leica Ultracut equipped with a FCS cryoattachment operating at −100°C. Sections were floated successively on PBSFCS, anti-MIC4, or anti-MIC6 rabbit antiserum diluted 1:40 in PBSFCS, 8 nm protein A–gold diluted to 0.05 OD 525 nm in PBS, with 5 × 3 min washings in PBS between each step. Detections with anti-MIC1 or anti-SAG1 mAbs included an additional step with anti–mouse immunoglobulin antiserum followed by protein A–gold. Sections were embedded in methylcellulose (2%)-uranyle acetate (0.4%) and observed with a Philips EM 420 electron microscope.

Results

Disruption of MIC1, MIC4, and MIC6 Genes by Double Homologous Recombination

Micronemal proteins have a modular structure composed of diverse adhesive domains. A schematic representation of the micronemal proteins analyzed in this study is depicted in Fig. 1 A, and the postexocytosis processing events on these proteins are indicated by arrows. These proteolytic cleavages occur on the parasite surface, upon release by the micronemes, except for MIC3 and MIC6. We have previously shown that MIC6 is processed at the NH_2 terminus during its transport to the micronemes, whereas cleavage at the COOH terminus takes place after discharge by the organelles (Meissner et al., unpublished results).

To investigate the function of the micronemal proteins in *T. gondii*, we have generated mutant parasite cell lines in which *MIC1*, *MIC4*, or *MIC6* genes have been disrupted by gene replacement. The vectors used to generate these knockouts contained ≥1,500 bp of homologous sequences corresponding to the 5′ and 3′ flanking sequences of *MICs* genes. The selectable marker gene cassette used in those experiments was *HXGPRT* controlled by *DHFRTS* flanking sequences (Donald and Roos, 1998). Parasite clones resistant to mycophenolic acid were examined for the absence of MIC1, MIC4, or MIC6, respectively, by IFA. 10–20% of the resistant clones appeared to have recombined homologously in the case of MIC4 and MIC6. One clone of mic1ko, mic4ko, and mic6ko were kept for further analysis. The absence of MIC1, MIC4, and MIC6 proteins in mutant cell lines was confirmed by Western blot analysis. The rabbit serum anti-MIC4 and the antisera raised against the CD of MIC6 recognized two bands corresponding to processed forms of MIC4 and MIC6, respectively. In the knockout strains, both signals disappeared, confirming that the two forms are indeed processed forms of the same gene products (Fig. 2). Southern blot analysis established that disruption of these three micronemal genes occurred by double homologous recombination events (data not shown).

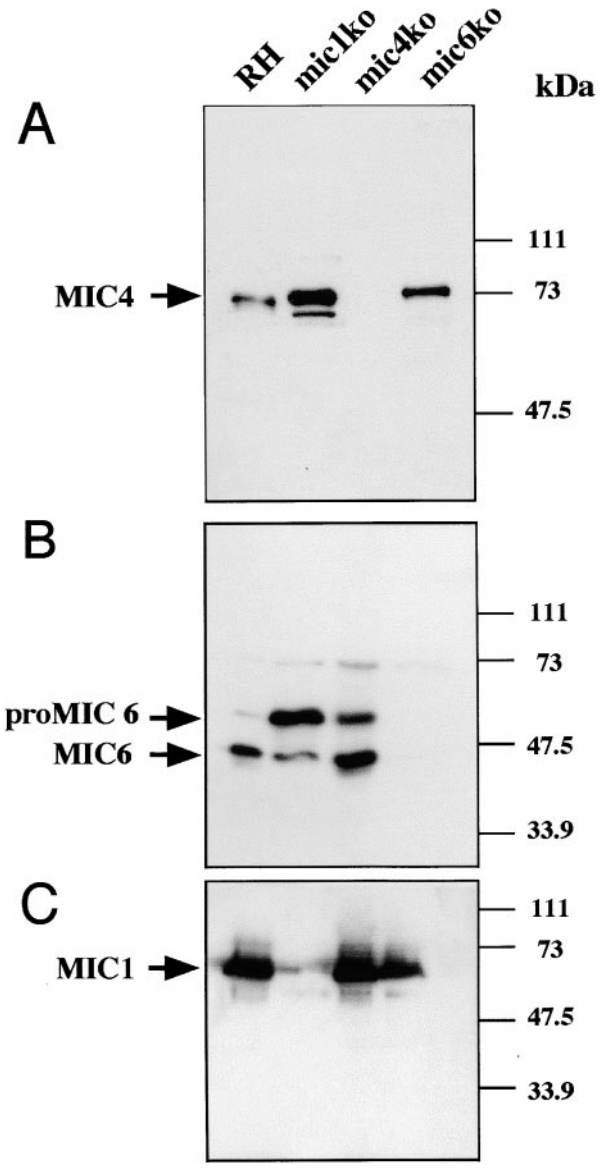

Figure 2. Disruption of *MIC1*, *MIC4*, and *MIC6* genes in *T. gondii* tachyzoites by double homologous recombination. Western blot analysis of an equal loading of whole cell lysates corresponding to 5 × 10^6 tachyzoites from RH, mic1ko, mic4ko, and mic6ko. In A–C, membranes were probed with rabbit antibodies anti-MIC4, anti-MIC6, and mAb anti-MIC-1, respectively.

Figure 3. MIC1 and MIC4 are mistargeted in mic6ko and accumulate in the dense granules and the parasitophorous vacuole. (A) Mistargeting of MIC1 and MIC4 was analyzed by confocal microscopy of HFF cells infected with mic6ko and compared with RH. In wild-type parasites, T101F7 mAb anti-MIC1 and polyclonal anti-MIC4 showed perfect colocalization of the two proteins and a typical apical micronemes staining. In contrast, MIC4 did not colocalize with the other micronemal protein MIC2 (mAb T34A11) in mic6ko parasites but instead accumulated in dense granules and in the parasitophorous vacuolar space. Under mild fixation conditions, the vacuolar signal of MIC4 is lost, and the remaining MIC4 colocalizes with the dense granule marker GRA3 (mAb T26H11, in red). (B) The vacuolar accu-

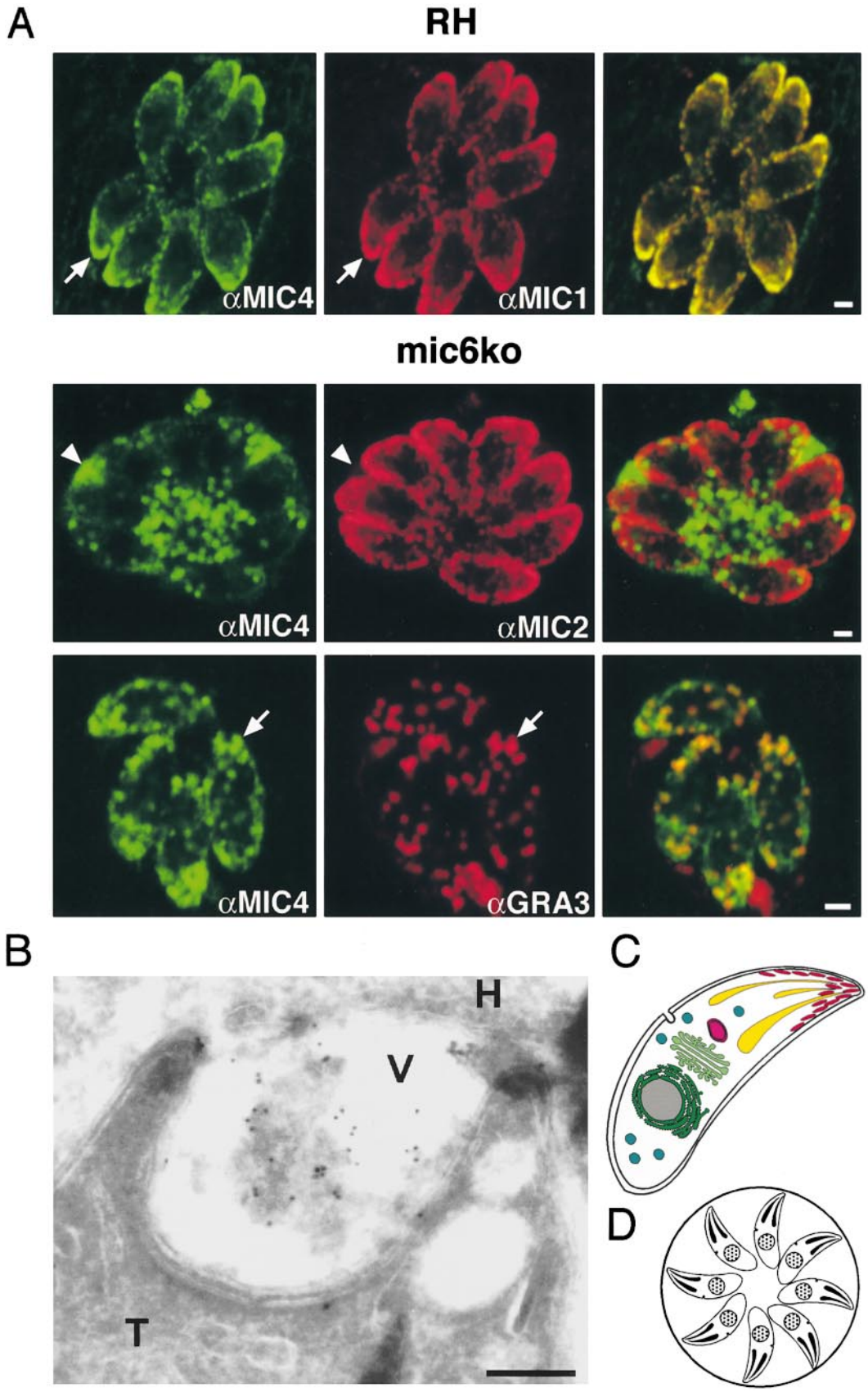

mulation of MIC4 in mic6ko was confirmed by immunolocalization of MIC4 in mic6ko. The label is over the dense material found at the posterior end of a tachyzoite fixed early after invasion, typical of dense granules exocytosis. T, tachyzoite; V, parasitophorous vacuole; H, host cell. (C) Schematic representation of the secretory pathway in a tachyzoite. The nucleus (gray), the ER (dark green), the Golgi apparatus (light green), the apicoplast (pink), the dense granules (blue), the rhoptries (yellow), and the micronemes (red). (D) Schematic representation eight parasites arranged in rosette within the parasitophorous vacuole after three cell divisions. Bars: (A) 1 μm; (B) 0.2 μm.

Absence of MIC6 Protein Causes Complete Mistargeting of the Two Soluble Micronemal Proteins MIC1 and MIC4

Recombinant parasites lacking MIC6 (mic6ko) showed normal growth and appeared to bind and invade HFF cells like the parent strain in the cell culture conditions tested so far. Upon analysis of other micronemal proteins by IFA, we observed that two soluble proteins MIC1 and MIC4 failed to accumulate in the micronemes in absence of MIC6. Instead, as shown in Fig. 3 A (and see Fig. 5 A), both MIC1 and MIC4 are rerouted into the default secretory pathway, which in *T. gondii* traffics through the dense granules and ends in the parasitophorous vacuole (Karsten et al., 1998). Mild fixation protocols were used to visualize the presence of MIC4 and its colocalization with GRA3 in the dense granules (Bermudes et al., 1994). In contrast, the transmembrane protein MIC2 and two other micronemal proteins exhibiting no putative transmembrane domain, MIC3 (Garcia-Réguet et al., 2001), or MIC5 (Brydges et al., 2000) were faithfully targeted to the micronemes in mic6ko (data not shown). Analysis of the mic6ko by transmission electron microscopy confirmed the unprecedented localization of the micronemal proteins MIC4 (Fig. 3 B) and MIC1 (not shown) in the parasitophorous vacuolar space. The distinct compartments of the secretory pathway in *T. gondii* are schematically drawn in Fig. 3 C. After few divisions by endodyogeny, the parasites are organized in rosette within the parasitophorous vacuole (Fig. 3 D).

The Cytoplasmic Tail of MIC6 Contains a Microneme-targeting Signal(s)

Mistargeting of MIC1 and MIC4 in absence of MIC6 implies that MIC6 carries sorting signals to the micronemes. A recent study in *T. gondii* has demonstrated the existence of tyrosine-based sorting signals, the corresponding machinery, and their involvement in the targeting of proteins to the rhoptries (Hoppe et al., 2000). In parallel, a mutagenesis analysis of the CD of MIC2 has revealed that two conserved motifs are both necessary and sufficient for targeting proteins to the micronemes (Di Cristina et al., 2000). One of these signals contains tyrosine residues, whereas the other one is composed of a stretch of acidic residues. Both motifs are also present and strictly conserved in the CD of MIC6. We have replaced the GPI-anchoring signal in the major surface antigen SAG1 with the transmembrane and CDs of MIC6 (TM-CD^{MIC6}) and have expressed stably SAG1TM-CD^{MIC6} in the mic6ko parasites (Fig. 1 B). Deletion of the GPI anchor signal led to the accumulation of soluble SAG1 in the parasitophorous vacuole (data not shown). In contrast, SAG1TM-CD^{MIC6} localized essentially to the micronemes, as detected by IFA with antibodies specific for the CD of MIC6 (Fig. 4 A). The expression of SAG1TM-CD^{MIC6} failed to restore the mic6ko phenotype since both MIC1 and MIC4 still accumulated in the vacuolar space and are absent from micronemes, as evident from the lack of colocalization with MIC2 (Fig. 4 A). Immunoelectron microscopy analysis of parasites expressing SAG1TM-CD^{MIC6} with anti-SAG1 mAbs demonstrated SAG1 reactivity in micronemes, in addition to its normal location at the parasite surface (Fig. 4 B).

MIC6 Is Associated to MIC1 and MIC4

The results described above suggested that MIC6 is interacting with MIC1 and MIC4 and thus its presence is prerequisite for the accurate targeting of these two soluble proteins to the micronemes. To confirm that MIC6 fulfills this function and that indeed the absence of MIC6 only was responsible for the observed phenotype, we reintroduced the full-length MIC6 carrying a Ty-1 epitope tag (MIC6Ty-1; Fig. 1 B) into mic6ko strain. MIC6Ty-1 accumulated to the micronemes and was able to fully rescue the missorting phenotype of MIC1 (Fig. 5 A) and MIC4 (data not shown). Two additional mutant constructs of MIC6 were integrated into mic6ko and provided compelling evidence that MIC6 interacts directly with MIC1 and MIC4 via its lumenal domain. Deletion of the CD of MIC6 produces a truncated protein, MIC6ΔCD, which lacks sorting signals and is retained predominantly in the perinuclear region (Fig. 5 B). Under these circumstances, both MIC1 and MIC4 were retained in the same compartment as MIC6ΔCD. The best evidence for a physical association between the three MICs was obtained when the TM-CD^{MIC6} were replaced by the GPI anchoring signal of SAG1. In this case, the GPI anchorage of MIC6GPI occurs in the ER, and the chimeric protein is efficiently targeted to the plasma membrane, likely via the constitutive secretory pathway (Karsten et al., 1998). As expected, MIC6GPI localized perfectly at the plasma membrane as seen by IFA on nonpermeabilized extracellular parasites (data not shown), and on permeabilized intracellular parasites (Fig. 5 C). In mic6ko expressing MIC6GPI, both MIC1 and MIC4 were efficiently transported to the parasite surface where they remained tightly associated with the parasite membrane without diffusing in the vacuolar space (Fig. 5 C). Interestingly, the unusual presence of these three micronemal proteins at the plasma membrane dramatically increased the stickiness of the parasites, which showed a high tendency to aggregate after release from their host cells (data not shown). Western blot analysis of recombinant parasites confirmed that MIC6Ty-1 had the appropriate size and was correctly processed both at the NH_2 and COOH terminus (Fig. 5 D). Similarly, MIC6GPI has the expected mobility on SDS-PAGE and appeared to be faithfully processed at the NH_2 terminus (Fig. 5 D). The migration of MIC6ΔCD did not allow identifying without ambiguity if processing had occurred. These results provided additional evidence that the NH_2-terminal processing of MIC6 occurred in the TGN rather than in the micronemes, since MIC6GPI is not expected to traffic through these organelles. This approach provided compelling genetic evidence for a stable direct or indirect interaction between MIC6, MIC1, and MIC4.

MIC1, MIC4, and MIC6 Interact Physically

Evidence for the existence of a complex between MIC1, MIC4, and MIC6 was confirmed and supported biochemically by coimmunoprecipitation experiments. Parasite lysates were prepared under mild conditions by sonification and subjected to immunoprecipitation with mAb anti-MIC1. Western blot analysis revealed that both MIC4 and MIC6 coprecipitated (Fig. 6 A). Interestingly, the two processed forms of MIC6 coimmunoprecipitated with anti-

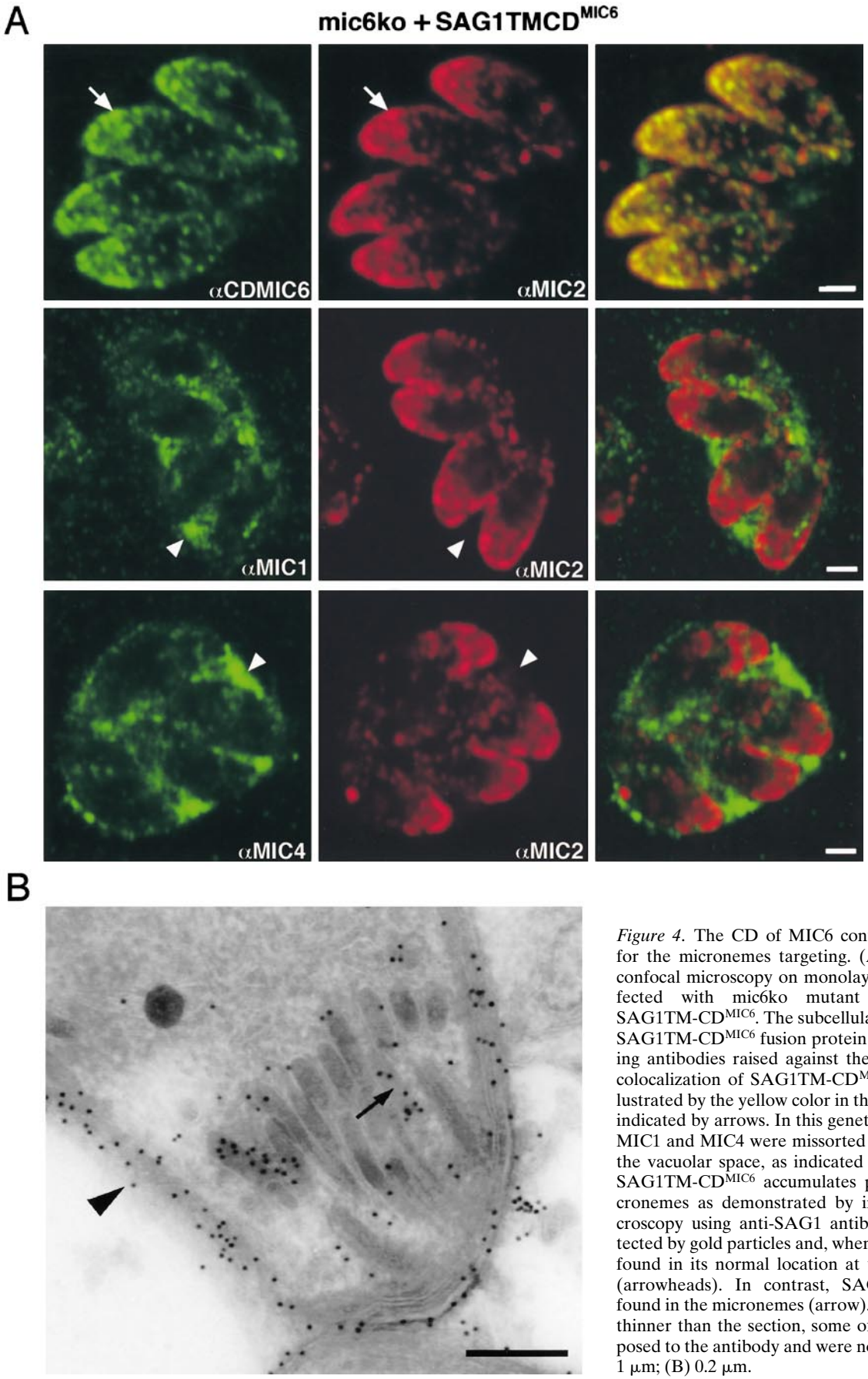

Figure 4. The CD of MIC6 contains sorting signals for the micronemes targeting. (A) IFA analysis by confocal microscopy on monolayers of HFF cells infected with mic6ko mutant expressing stably SAG1TM-CD^{MIC6}. The subcellular distribution of the SAG1TM-CD^{MIC6} fusion protein was detected by using antibodies raised against the CD of MIC6. The colocalization of SAG1TM-CD^{MIC6} with MIC2 is illustrated by the yellow color in the merged image and indicated by arrows. In this genetic background, both MIC1 and MIC4 were missorted and accumulated in the vacuolar space, as indicated by arrowheads. (B) SAG1TM-CD^{MIC6} accumulates precisely in the micronemes as demonstrated by immunoelectron microscopy using anti-SAG1 antibodies. SAG1 is detected by gold particles and, when GPI anchored, was found in its normal location at the parasite surface (arrowheads). In contrast, SAG1TM-CD^{MIC6} was found in the micronemes (arrow). As micronemes are thinner than the section, some of them were not exposed to the antibody and were not labeled. Bars: (A) 1 μm; (B) 0.2 μm.

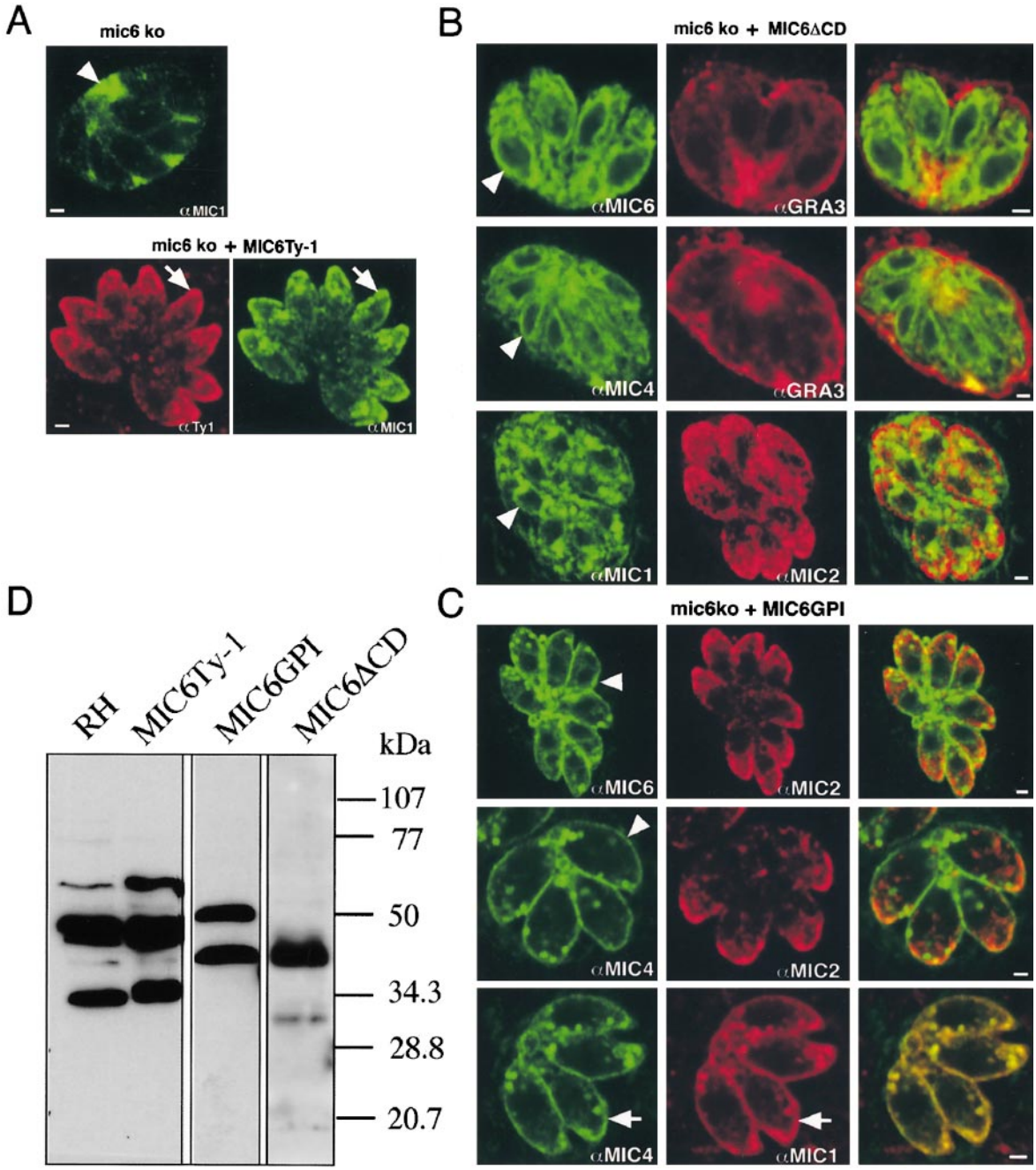

Figure 5. Rescue of mic6ko and evidence for a direct interaction between MIC1 MIC4 and MIC6. (A) Subcellular distribution of endogenous MIC1 and MIC6Ty-1 were analyzed by confocal microscopy in mic6ko and mic6ko expressing MIC6Ty1. The missorting of MIC1 to the vacuolar space (arrowhead) in mic6ko was reverted in mic6ko expressing MIC6Ty-1. MIC6Ty-1 localized to the micronemes as detected by mAb anti-Ty1 (arrows). (B) Expression of pTMIC6ΔCD in mic6ko was analyzed by IFA using anti-MIC6 raised against the EGF domains. MIC6ΔCD lacking the microneme sorting signals was retained in a perinuclear region (arrowheads). Similarly, endogenous MIC1 and MIC4 accumulated in the same compartments. The absence of accumulation of MIC4 in the vacuolar space or MIC1 targeting to the micronemes were observed by double IFA with the two markers GRA3 and MIC2, respectively. (C) MIC6GPI is covalently linked to a GPI and, as a consequence, anchored at the plasma membrane (arrowhead) of the parasites in mic6ko. The localization of MIC6GPI at the plasma membrane caused the quantitative redistribution of endogenous MIC1 and MIC4 to the surface of the parasites (arrowheads). MIC6GPI and MIC4 were excluded from the micronemes as seen by the lack of colocalization with MIC2. Moreover, MIC1 and MIC4 colocalized perfectly. (D) RH and transformed parasites expressing MIC6Ty-1, MIC6GPI, and MIC6ΔCD were analyzed by Western blot with anti-MIC6. The two processed forms of MIC6 detectable in RH were also present in the rescued parasites expressing MIC6Ty-1. Two forms of MIC6GPI are detectable suggesting that the NH_2-terminal processing occurred. Bars, 1 μm.

MIC1, strongly suggesting that the complex is present both in the micronemes and at the surface of the parasites, where the COOH-terminal processing of MIC6 takes place. Coimmunoprecipitation experiments using mic6ko parasites clearly indicated that an interaction exists between MIC1 and MIC4 even in the absence of MIC6 (Fig. 6 B). Cell lysates from mic1ko parasites expressing MIC1myc were used to demonstrate that the polyclonal anti-CDMIC6 can coimmunoprecipitate MIC1 and MIC4 as detected on immunoblot using the mAb anti-myc 9E10 and the mAb anti-MIC4 5B2 (Fig. 6 C). Finally, the polyclonal anti-NtMIC6 also coimmunoprecipitated MIC4 in lysates from wild-type parasites (Fig. 6 D). Together, these data provided complementary information with regard to the topology of the complex, which is schematically depicted in Fig. 6 E.

The Third EGF-like Domain (EGF-3) of MIC6 Is Involved in the Sorting of MIC4 and MIC1

MIC6 mutants with various deletions in their lumenal domains were generated and stably expressed in the mic6ko strain. Phenotypic analysis of these mutants by IFA allowed identifying the domain on MIC6, interacting with MIC1 and MIC4. MIC6 mutants lacking either the three EGF domains or the acidic domain were poorly targeted to the micronemes. These large deletions are likely to cause significant alteration of the folding properties of the

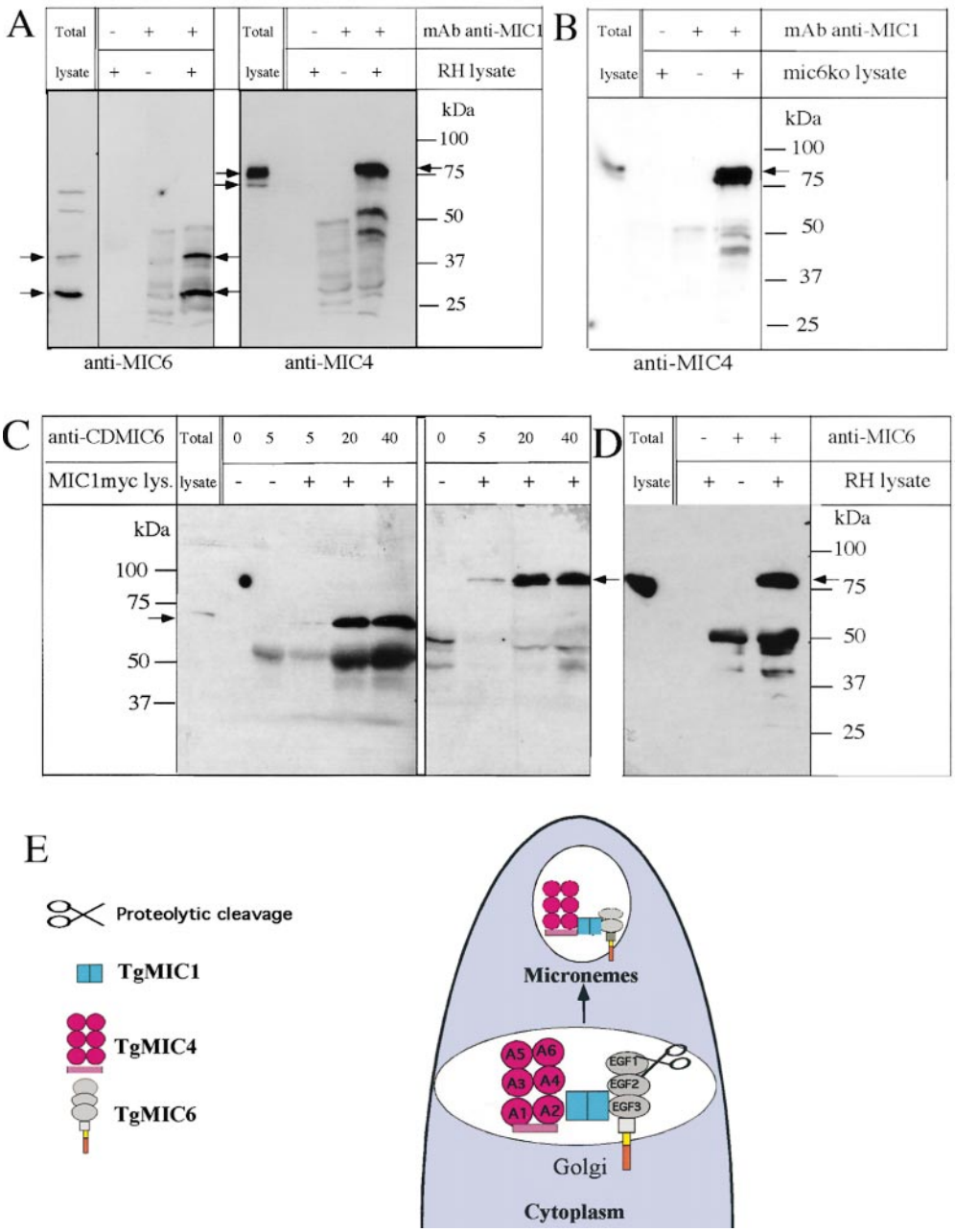

Figure 6. MIC1, MIC4, and MIC6 physically interact. (A) Immunoprecipitation of a complex containing MIC1, MIC4, and MIC6 from wild-type parasite lysate (RH lysate) by anti-MIC1 mAbs. The immunoprecipitates were shown to contain also MIC6 and MIC4 by Western blot analysis using rabbit polyclonals anti-MIC6 or anti-MIC4. The two processed forms of MIC6 and the two forms of MIC4 are indicated by arrows. Controls included immunoprecipitation in absence of lysate or in absence of the mAb anti-MIC1. (B) Coimmunoprecipitation of MIC4 with anti-MIC1 in cell lysates of mic6ko parasites showed that they interact in absence of MIC6. (C) Coimmunoprecipitation of MIC1 (detected with mAb anti-myc) and MIC4 using the polyclonals anti-CDMIC6 from lysates of mic1ko parasites expressing MIC1myc. The immunoprecipitation was carried out with increasing amount of antibodies (5, 20, and 40 μl). (D) Coimmunoprecipitation of MIC4 with anti-MIC6 from RH lysate. (E) Model. A complex between MIC1, MIC4, and MIC6 forms in the early compartments of the secretory pathway and ensures the proper targeting of MIC1 and MIC4 to the micronemes via the interaction of MIC6 cytoplasmic tail with the sorting machinery. During its transport, MIC6 is processed at the NH_2 terminus and looses the first EGF-like domain. Upon contact with host cells, an increase in free intracellular calcium stimulates the discharge of the microneme contents. The complex of MICs is liberated at the surface of the parasites, potentially anchored within the plasma membrane via MIC6.

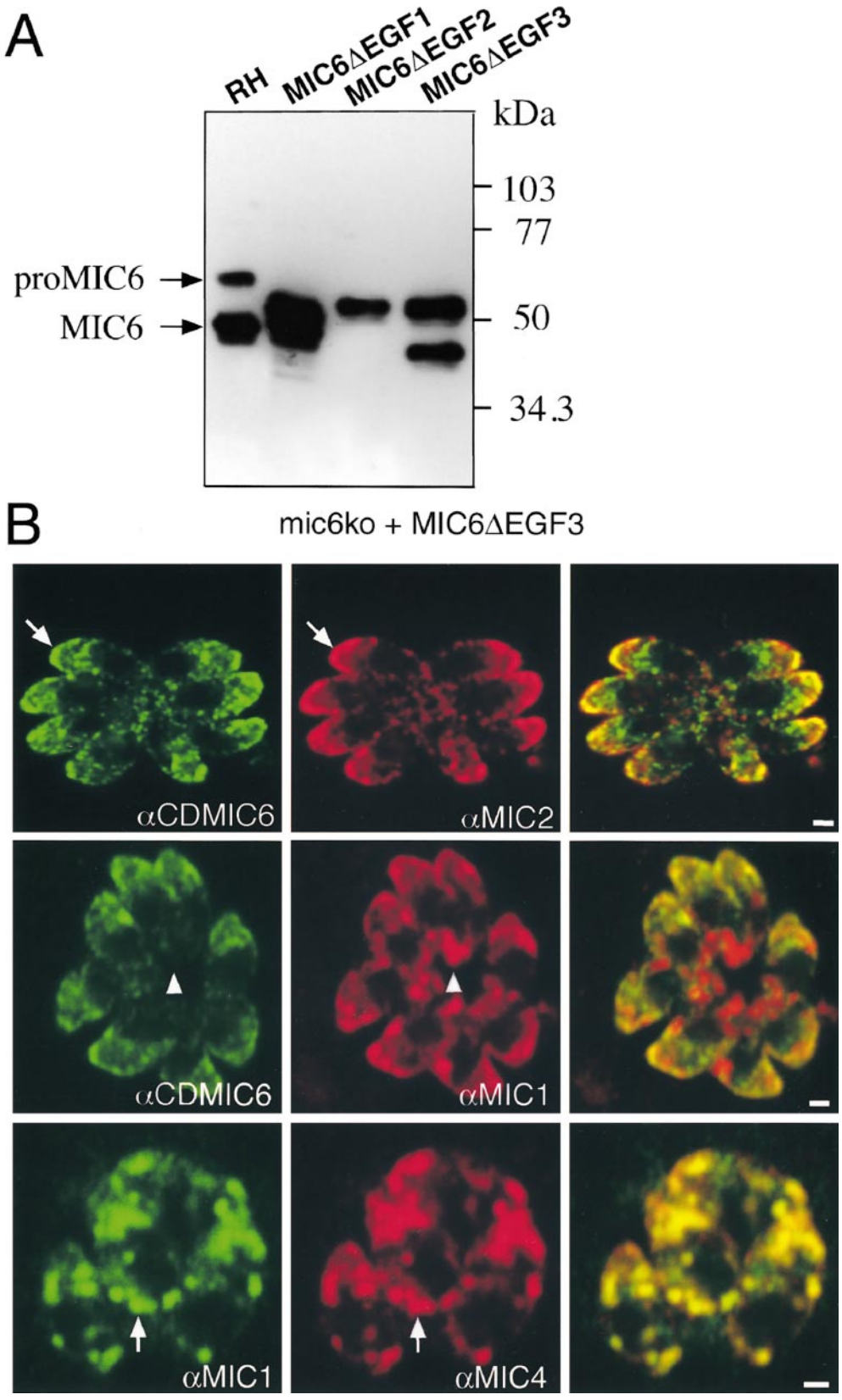

Figure 7. The EGF-3 domain of MIC6 is necessary for accurate targeting of MIC1 and MIC4 to the micronemes. (A) Western blot analysis of cell lysates from RH and recombinant parasites expressing MIC6ΔEGF1, MIC6ΔEGF2, and MIC6ΔEGF3 with anti-CDMIC6 antibodies (raised against the CD of MIC6). MIC6ΔEGF1 and MIC6ΔEGF3 were still subjected to NH_2-terminal cleavage, whereas a single form of MIC6ΔEGF2 was detectable, suggesting that the cleavage site has been deleted by removing the EGF-2 domain. (B) IFA analysis by confocal microscopy. MIC6ΔEGF-3 expressed in mic6ko was accurately targeted to the micronemes, as detected with anti-CDMIC6, and colocalized with MIC2 (arrows). In this mutant, MIC4 was only partially sorted to the micronemes (arrowhead), with a significant amount of protein still accumulating in the dense granules. MIC1 and MIC4 colocalized (arrows). Bar, 1 μm.

truncated proteins. However, more subtle deletions of each individual EGF-like domain produced truncated proteins that were perfectly targeted to the organelle. Western blot analysis of the deletion mutants using the anti-MIC6 tail demonstrated that the MIC6 mutants were expressed at comparable levels (Fig. 7 A). The migration behavior of the various mutants and the absence of processing on MIC6ΔEGF-2 indicated that the NH_2-terminal cleavage of MIC6 occurred within the second EGF domain. The subcellular distribution of MIC1 and MIC4

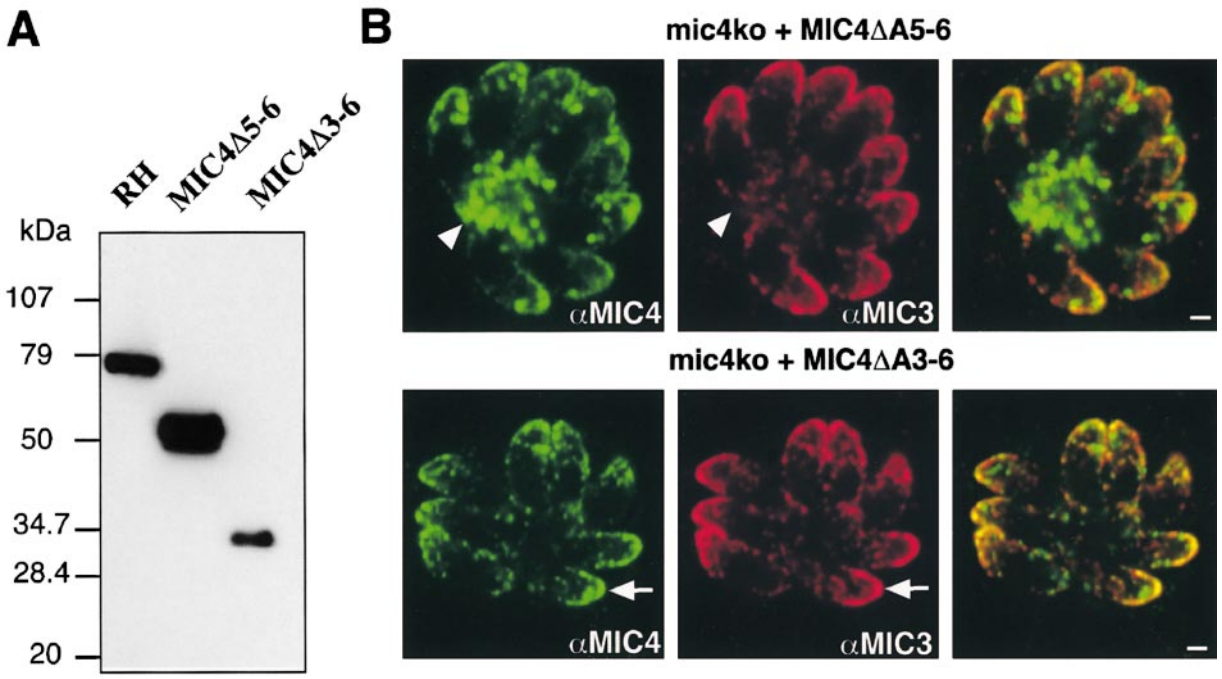

Figure 8. Expression of MIC4 deletion mutants in mic4ko. The NH_2-terminal region of MIC4 containing the first two apple domains was correctly sorted to the micronemes. (A) Western blot analysis of cell lysates from RH and recombinant parasites expressing MIC4ΔA5-6 or MIC4ΔA3-6. The migration of MIC4 and the truncated forms on SDS-PAGE were slower than their predicted molecular weight. (B) IFA analysis by confocal microscopy of parasites expressing MIC4ΔA5-6 and MIC4ΔA3-6. Proper targeting to the micronemes was confirmed by colocalization with MIC3. Bar, 1 μm.

in these mutants was analyzed by IFA. In summary, MIC6ΔEGF-1 and MIC6ΔEGF-2 were able to fully rescue the missorting phenotype, with both MIC1 and MIC4 faithfully targeted to the micronemes (data not shown). In contrast, in parasites expressing MIC6ΔEGF-3, neither MIC1 nor MIC4 were quantitatively sorted to the micronemes, although MIC6ΔEGF-3 localized to these organelles as shown by colocalization with MIC2 (Fig. 7 B). These results suggest that the EGF-3 domain is necessary for an efficient interaction of MIC6 with MIC1 and MIC4 individually or with one of the two, whereas MIC1 and MIC4 are directly associated. A possible contribution of the adjacent acidic domain can not be excluded by this analysis.

MIC4 Is a Passive Cargo Protein and Two Apple Domains at the NH_2 Terminus Are Sufficient to Target the Protein to the Micronemes

To assess the contribution of each partner in the complex, we have abrogated selectively their expression. *MIC4* cDNA has a predicted ORF of 580 amino acids that contains a single NH_2-terminal hydrophobic region. The protein contains six apple domains comprising six cysteine residues separated by variable spacing that are predicted to form a structure resembling an apple (McMullen et al., 1991a,b). Homologues of this protein have been identified in *Spironucleus muris* and in *Eimeria* species (Brown et al., 2000). The protein is an adhesin, which is proteolytically cleaved both at the NH_2 and COOH terminus at the surface of the parasite after release from the micronemes (Brecht et al., 2001). The level of expression and subcellular distribution of the other micronemal proteins was carefully examined in the mic4ko. We concluded that all micronemal proteins described in *T. gondii* so far were appropriately expressed and sorted in this mutant (data not shown). The correct targeting of MIC1 in absence of MIC4 testified for a direct association of MIC1 with MIC6, excluding an association via MIC4. Two deletion mutants of MIC4 lacking the last two, MIC4ΔA5-6, or the last four apple domains, MIC4ΔA3-6 (Fig. 1 B) were generated and expressed stably in the mic4ko recipient strain. These clones were analyzed by Western blotting and showed products of the expected sizes (Fig. 8 A). IFA analysis of these mutants confirmed that the truncated proteins lacking the NH_2-terminal two or four apple domains were still localized to the micronemes and have consequently retained the ability to associate with MIC1 (Fig. 8 B). The MIC4ΔA5-6 mutant was substantially overexpressed compared with MIC4 in wild type, causing a significant spill over of the truncated protein into the default pathway leading to an accumulation of the protein into the dense granules, as perceptible on IFA.

MIC1 Is Necessary for MIC6 and MIC4 to Leave the Golgi

MIC1 localizes to micronemes and has been shown to bind to host cells (Fourmaux et al., 1996). *MIC1* gene encodes a polypeptide of 456 amino acids containing two domains bearing some homology to the thrombospondin domains present in the TRAP family (Naitza et al., 1998). The absence of *MIC1* gene is not essential for the survival of the parasites in culture, and, like in mic4ko, the targeting of other micronemal proteins was investigated in the mic1ko strain. Unlike MIC4, the absence of MIC1 has a drastic and specific effect on the sorting of the two other members

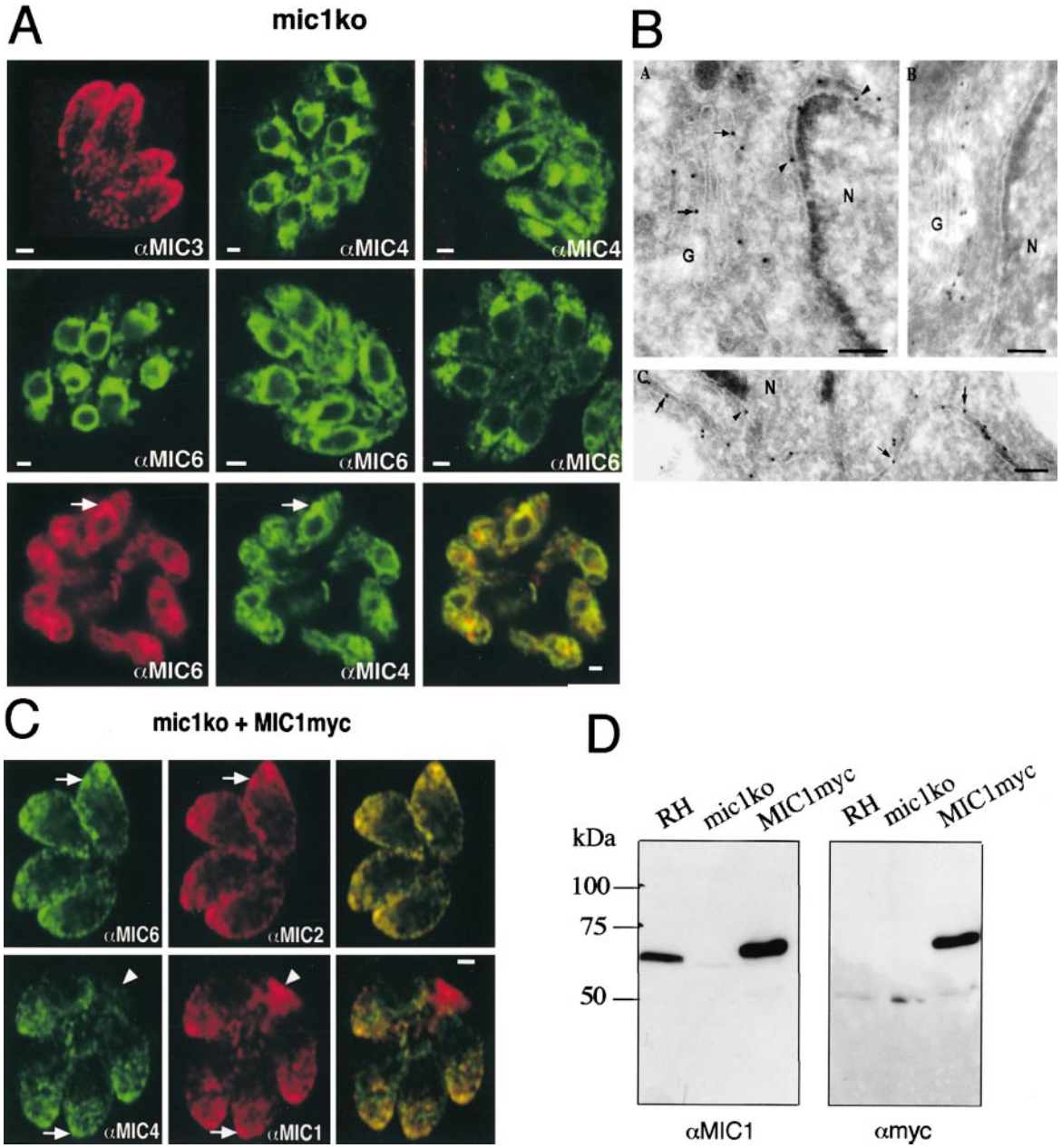

Figure 9. Analysis of mic1ko. MIC1 is necessary for MIC6 and MIC4 to leave the ER and Golgi. (A) Subcellular distribution of MIC4 and MIC6 in mic1ko strain analyzed by IFA. MIC3 was faithfully sorted to the micronemes, whereas MIC4 and MIC6 were retained in the early compartments of the secretory pathway. Two vacuoles stained with anti-MIC4 and three vacuoles stained with anti-MIC6 are presented here to illustrate the various compartments where the two proteins are retained. A double IFA of MIC4 and MIC6 in mic1ko indicated that in all vacuoles, both proteins colocalized perfectly as shown in the merged image. (B) Immunolocalization of MIC6 and MIC4 in mic1ko by electron microscopy revealed various patterns of distribution in the early secretory compartments. (A) MIC4 was detected in the nuclear envelope (arrowheads) and in the successive stacks of the Golgi (arrows). N, nucleus; G, Golgi apparatus. (B) MIC6 stagged in the cis-Golgi. (C) MIC4 stagged in the ER (arrows) and nuclear envelope (arrowheads). (C) The mic1ko mutant expressing MIC1myc showed rescue of the phenoptype by IFA. In presence of MIC1myc, both MIC4 and MIC6 were quantitatively sorted to the micronemes. A slight overexpression of MIC1 led to some leakage to the vacuolar space as detected by anti-MIC1 mAb. (D) Western blot analysis of lysates form RH, mic1ko, and mic1ko complemented with MIC1myc using either anti-MIC1sera or anti-myc mAb. A slight increase in the size of MIC1myc was apparent compared with endogenous MIC1, due to the presence of the myc tag. Bars: (A and C) 1 μm; (B) 0.2 μm.

of the complex. In absence of MIC1, both MIC2 and MIC3 are properly localized in the micronemes, whereas MIC4 and MIC6 are retained in the early compartments of the secretory pathway. A selective accumulation of these proteins in the perinuclear region, ER, Golgi, and possibly TGN was observed. Within each single vacuole, all the parasites showed a homogeneous distribution in a particular compartment of the secretory pathway, whereas the distribution varied between vacuoles. The heterogeneity of staining observed within the population of vacuoles is

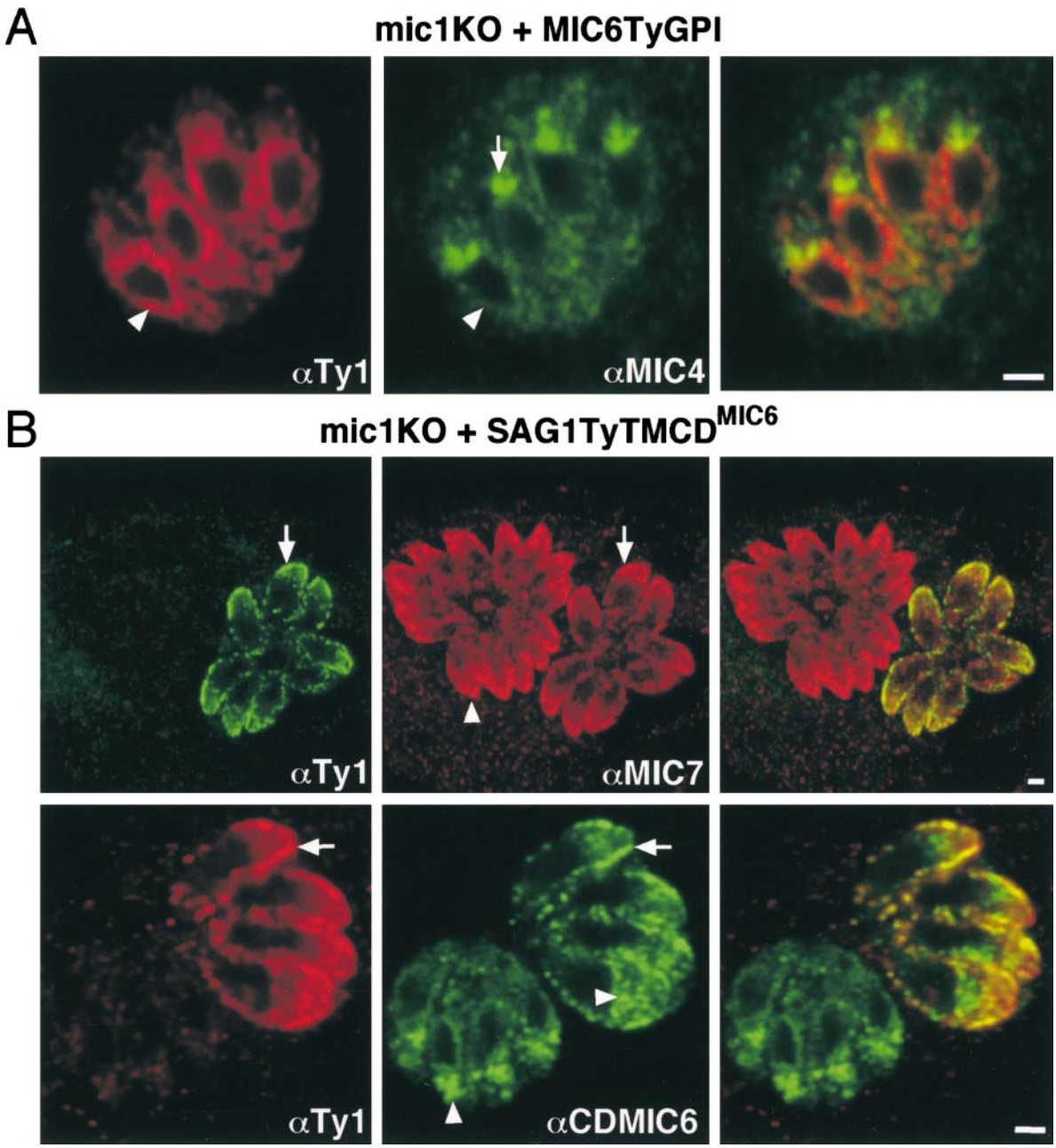

Figure 10. Trafficking of MIC6GPI and SAG1TM-CD^{MIC6} in mic1ko. Pools of parasites expressing MIC6TyGPI and SAG1Ty1TM-CD^{MIC6} were analyzed by IFA. (A) MIC6TyGPI localized predominantly to the perinuclear region as detected by the anti–Ty-1 antibodies (arrowhead). The endogenous MIC4 was retained in the early compartments of the secretory pathway (arrow). (B) SAG1TM-CD^{MIC6} was accurately sorted to the micronemes as shown by the extensive colocalization with the microneme marker MIC7 (rabbit polyclonal anti-MIC7 raised against the EGF-like domains; Meissne, M., and D. Soldati, unpublished results). The vacuole on the left was not transformed with SAG1TM-CD^{MIC6} and showed the absence of background with the mAb anti-Ty-1. The pool of transformants was analyzed with the anti-CDMIC6 revealing that the endogenous MIC6 (green, arrows) is retained in the ER and Golgi. Bar, 1 μm.

suggestive of a cell cycle–dependent effect. Fig. 9 A shows retention of MIC4 and MIC6 in various compartments of the secretory pathway. Analysis by immunoelectron microscopy confirmed the localization of MIC4 in the Golgi stacks and ER (Fig. 9 B). In all circumstances, MIC4 and MIC6 perfectly colocalized, and we failed to identify a single vacuole with a MIC4 or MIC6 localized to the micronemes. A complete rescue of this phenotype was observed by IFA when mic1ko were stably transformed with the vector pM2MIC1myc (Fig. 9 C). Expression of MIC1myc fully restored the transport of MIC4 and MIC6 to the micronemes. In this mutant, MIC1 did not only accumulate in the micronemes, but a small proportion of it also transited via the dense granules and reached the parasitophorous vacuole. This result suggests that MIC6 is present in limiting amount, and when this escorter becomes saturated, both MIC1 and MIC4 are missorted. Western blot analysis of the mic1ko rescue showed that the reintro-

duced MIC1myc was slightly overexpresssed compared with MIC1 in RH (Fig. 9 D). MIC6 in mic1ko indicated that retention of MIC6 in the early compartments of the secretory pathway correlated with the accumulation of the unprocessed form of the protein (Fig. 2 B). In the rescued mutant expressing MIC1myc, the ratio between full-length MIC6 and the NH_2-terminal processed form is restored as in wild type (data not shown).

Trafficking of MIC6GPI and SAG1TM-CD^{MIC6} in mic1ko

The absence of MIC1 is expected to interfere with the trafficking of the lumenal part of MIC6, whereas the CD of MIC6 should not be affected. To test this hypothesis, we have generated constructs, the MIC6TyGPI and SAG1TyTM-CD^{MIC6}, to follow their expression in mic1ko strain. The presence of a Ty-1 tag allowed us to unambiguously distinguish the transgenes from the endogenous MIC6 and SAG1. These constructs were introduced stably in mic1ko by cotransfection with a plasmid expressing CAT gene as selectable marker, and pools of transformants were analyzed by IFA. As opposed to the plasma membrane localization of MIC6GPI in wild-type parasites (data not shown) and in mic6ko (Fig. 5 D), MIC6TyGPI expressed in mic1ko was retained predominantly in the ER and to a lesser extent in the Golgi compartments (Fig. 10 A). In this genetic background, endogenous MIC4 is still retained in the early compartments of the secretory pathway and MIC6 (data not shown). In contrast, the trafficking of SAG1TyTM-CD^{MIC6} (Fig. 1 B) in mic1ko was not affected, confirming the MIC1 acts on the lumenal part of MIC6. As expected, SAG1TyTM-CD^{MIC6} colocalized perfectly with another micronemal marker, MIC7 (Meissner et al., unpublished results) (Fig. 10 B). Detection of the SAG1TyTM-CD^{MIC6} in mic1ko using the polyclonal antibody anti-CDMIC6 confirmed that the endogenous MIC6 is still retained in the early secretory pathway in this mutant.

Discussion

The mechanism by which regulated secretory proteins are sorted has been intensively studied in higher eukaryotic cells. Transmembrane proteins exhibit critical tyrosine residues in their cytoplasmic tails, which facilitate their sorting by binding to the cytoplasmic adaptor complexes that, together with coat components, assist vesicular transport (Marks et al., 1997; Hirst and Robinson, 1998). Tyrosine-based sorting signals and the associated machinery exist in *T. gondii* and are involved in the sorting to the specialized secretory organelles, called rhoptries (Hoppe et al., 2000). In this study, we show that the short cytoplasmic tail of MIC6 contains the information necessary and sufficient for sorting the surface protein SAG1 to the micronemes. A scanning mutagenesis analysis of the transmembrane protein MIC2 cytoplasmic tail has recently identified two sorting signals, which are also conserved in MIC6 tail (Di Cristina et al., 2000). Consistent with the importance of the tail in sorting, MIC6ΔCD lacking these signals was quantitatively retained in the ER/Golgi compartments. The MIC6 deletion mutant in which both the transmembrane and the cytoplasmic tail are deleted was also retained in the ER in wild-type parasites (data not shown). This observation implies that the presence of endogenous MIC6 failed to assist MIC6ΔCD in sorting to the micronemes, and thereby MIC6 is unlikely to form dimers.

In the case of soluble proteins, the lack of connection with the cytoplasm implies that a different mechanism for sorting must occur. A process of aggregation, condensation, and membrane association has been described for sorting soluble proteins into mammalian secretory granules (Glombik and Gerdes, 2000). The existence of specific membrane-spanning cargo receptors facilitating the sorting of soluble proteins has also been postulated and questioned (Thiele et al., 1997). In the present study, we demonstrate that MIC6 is required to escort accurately two soluble adhesins to the micronemes. We have been able to confirm the existence of a physical complex between MIC1, MIC4, and MIC6. Moreover, the fact that the interaction between MIC1 and MIC4 persists even in the absence of MIC6 provided valuable information with regard to the topology of this complex. MIC4 is likely associated to MIC6 via MIC1. The accumulation of MIC6GPI, MIC1, and MIC4 at the surface of the parasites firmly indicated that the environmental conditions (pH and Ca^{2+} concentration) do not significantly affect the stability of this complex, which might persist during invasion, when the micronemes exocytose their contents to the surface of the parasite.

The domains involved in the complex formation have been partially mapped in this study. The third EGF domain of MIC6 is essential for the accurate sorting of both MIC1 and MIC4. The presence of MIC4 is not required for correct sorting of MIC1, excluding the possibility that MIC1 interacts indirectly with MIC6 via MIC4. The deletion mutants of MIC4 showed that the two NH_2-terminal apple domains of MIC4 are sufficient for the sorting of the protein to the micronemes. The adhesive properties of MIC4 have been recently mapped to the most NH_2-terminal apple domain (Brecht et al., 2001). In contrast to MIC4, the absence of MIC1 has a drastic effect on its two partners, which are mostly retained in the ER/Golgi. MIC1 is indispensable for both MIC4 and MIC6 to leave the TGN and appears to hold the complex together. The massive retention caused by the absence of MIC1 suggests a connection with a quality control system of secretion in *T. gondii*. Interestingly, this phenomenon appears to apply to other apicomplexan parasite's secretory proteins since a recent study in *Plasmodium falciparum* showed that the absence of one rhoptry protein, RAP1, causes the retention in the ER and degradation of another rhoptry protein, RAP2 (Baldi et al., 2000). Retention can occur via exposed free cysteine residues and is referred to as thiol-mediated retention, implicating oxidoreductases responsible for retention of unassembled proteins (Frand et al., 2000). In that context, it is relevant to note that MIC4 and MIC6 are composed of apple and EGF-like domains, respectively, that are very rich in cysteine residues involved in disulfide bridge formation. The correct targeting of SAG1TyTM-CD^{MIC6} to the micronemes and the complete retention of MIC6GPI in the mic1ko background clearly confirmed that it is the lumenal region of MIC6, containing the EGF-like domains, that is implicated in this mecha-

nism. The processes of retention of MIC4 and MIC6 in the mic1ko and the precise role played by MIC1 remain to be investigated.

In a previous study, a combination of approaches suggested that in *T. gondii,* secretion from the ER to the Golgi uses the nuclear envelope as an intermediate compartment (Hager et al., 1999). In mic1ko, the population of vacuoles showed a heterogeneous distribution of MIC4 and MIC6 in discrete compartments along the secretory pathway. The nuclear envelope constitutes certainly one of the specific steps, corresponding to a defined compartment along the pathway. Since parasites are dividing synchronously within the vacuole, the accumulation of MIC4 and MIC6 in the ER and their subsequent vectorial transport are likely to be cell cycle dependent. Indeed some class of apical antigens, including micronemal proteins, have previously been reported to localize within the early compartments of the secretory pathway in a cell cycle–dependent fashion (Morrissette and Roos, 1998).

Some micronemal proteins are modified at the post-translational level by proteolytic cleavages (Achbarou et al., 1991; Brydges et al., 2000). Diverse processing events occur either during transport in the secretory pathway or after release by the micronemes and involve distinct proteases (Carruthers et al., 2000). The NH_2-terminal processing of MIC6 occurs before the protein reaches the micronemes, possibly in the TGN. The retention of MIC6 caused by the absence of MIC1 interferes with this process. However, the presence of the prosequence does not seem to be needed for the complex to leave the Golgi since the mutant MIC6ΔEGF-1 lacking most of the prosequence restored faithfully the mic6ko phenotype. The biological significance of this processing is still unclear.

MIC6 interacts specifically with MIC1 and MIC4 and escorts these adhesins to the micronemes with the assistance of the sorting signals, presumably interacting with adaptor complexes. The stoichiometry of the complex is not determined yet, but our data suggested that the MICs are present in roughly equimolar ratio. A slight overexpression of MIC4 or MIC1 leads to leakiness, whereas an overexpression of MIC6 causes its retention in the ER/Golgi. Beside its role as an escorter, MIC6 potentially plays a key function during invasion as a subunit of an adhesin complex. In wild-type parasites, the coimmunoprecipitation of the two processed forms of MIC6 with anti-MIC1 antibodies argues for the existence of a stable complex at the surface of the parasites. By anchoring the two adhesins to the surface of the parasites, MIC6 could establish a molecular bridge between the host and parasites. Its potential association with the host receptor–adhesin complexes would provide us with a satisfactory explanation as to how soluble adhesins can functionally contribute to host–cell parasite interaction. Consistent with a subsequent role during invasion, MIC6 possesses conserved amino acids in the cytoplasmic tail, including a tryptophan residue, like MIC2 and other members of TRAP family (Tomley and Soldati, 2001). The tail in PbTRAP is essential for motility and is anticipated to connect directly or indirectly with the actomyosin system of the parasite (Kappe et al., 1999). According to the capping model, the complex should redistribute towards the posterior pole of the parasites and, through the presence of the adhesins MIC1 and MIC4, contribute to gliding motility and host–cell invasion (Sibley et al., 1998).

We have thereby demonstrated for the first time in Apicomplexa that soluble secretory proteins are escorted to their target organelle through association with a transmembrane protein, which might in addition be a subunit of an adhesin complex. Like for the previous example of *P. falciparum* RAP1 and RAP2, this study reveals that secretory proteins can not be considered individually but rather as part of a network of interacting molecules. MIC6 belongs to a family of transmembrane micronemal proteins carrying EGF-like domains (Meissner et al., unpublished results), which leaves open the hypothesis that other members of this family are involved in the sorting of other sets of soluble adhesins. Indeed, preliminary data suggest that MIC7, an EGF-like containing transmembrane protein, influences the sorting of the soluble adhesin MIC3 (Meissner et al., unpublished results). Finally, it is surprising to realize that both the disruption of either MIC1 or MIC6 genes do not show significant alteration of invasiveness in vitro, despite the fact that these mutants are actually triple functional knockouts. These proteins may actually play a role at another parasite stage or be involved in some specific host–cell interaction in the host, or there is enough redundancy in parasite invasion to cope with this major deletion. Further studies will be needed to clarify this question.

We are indebted to Dr. Thierry Soldati for his stimulating and active participation in the project and his precious assistance at the confocal microscopy. We thank David Sibley for kindly providing us with the mAbs against MIC4. Special thanks Ursula Jäckle, Alexander Löwer, and Anne Loyens for their valuable technical assistance and the other members of the labs for critical reading of the manuscript.

This work was funded by the Deutsche Forschungsgemeinschaft (DFG grant SO 366/1-1, SO366/1-2) and by French Ministry of Research (PRFMMIP).

Submitted: 15 August 2000
Revised: 18 December 2000
Accepted: 18 December 2000

References

Achbarou, A., O. Mercereau-Puijalon, J.M. Autheman, B. Fortier, D. Camus, and J.F. Dubremetz. 1991. Characterization of microneme proteins of *Toxoplasma gondii. Mol. Biochem. Parasitol.* 47:223–233.

Baldi, D.L., K.T. Andrews, R.F. Waller, D.S. Roos, R.F. Howard, B.S. Crabb, and A.F. Cowman. 2000. RAP1 controls rhoptry targeting of RAP2 in the malaria parasite *Plasmodium falciparum. EMBO (Eur. Mol. Biol. Organ.) J.* 19:2435–2443.

Barnwell, J.W., and M.R. Galinski. 1995. *Plasmodium vivax*: a glimpse into the unique and shared biology of the merozoite. *Ann. Trop. Med. Parasitol.* 89: 113–120.

Bastin, P., Z. Bagherzadeh, K.R. Matthews, and K. Gull. 1996. A novel epitope tag system to study protein targeting and organelle biogenesis in *Trypanosoma brucei. Mol. Biochem. Parasitol.* 77:235–239.

Bermudes, D., J.F. Dubremetz, A. Achbarou, and K.A. Joiner. 1994. Cloning of a cDNA encoding the dense granule protein GRA3 from *Toxoplasma gondii. Mol. Biochem. Parasitol.* 68:247–257.

Brecht, S., V.B. Carruthers, D.J. Ferguson, O.K. Giddings, G. Wang, U. Jaekle, J.M. Harper, L.D. Sibley, and D. Soldati. 2001. The toxoplasma micronemal protein MIC4 is an adhesin composed of six conserved apple domains. *J. Biol. Chem.* In press.

Brown, P.J., K.J. Billington, J.M. Bumstead, J.D. Clark, and F.M. Tomley. 2000. A microneme protein from *Eimeria tenella* with homology to the apple domains of coagulation factor XI and plasma pre-kallikrein. *Mol. Biochem. Parasitol.* 107:91–102.

Brydges, S.D., G.D. Sherman, S. Nockemann, A. Loyens, W. Däubener, J.-F. Dubremetz, and V.B. Carruthers. 2000. Molecular characterization of TgMIC5, a proteolytically processed antigen secreted from the micronemes of *Toxoplasma gondii. Mol. Biochem. Parasitol.* 111:51–66.

Carruthers, V.B., G.D. Sherman, and L.D. Sibley. 2000. The Toxoplasma adhe-

sive protein MIC2 is proteolytically processed at multiple sites by two parasite-derived proteases. *J. Biol. Chem*. 275:14346–14353.

Dessens, J.T., A.L. Beetsma, G. Dimopoulos, K. Wengelnik, A. Crisanti, F.C. Kafatos, and R.E. Sinden. 1999. CTRP is essential for mosquito infection by malaria ookinetes. *EMBO (Eur. Mol. Biol. Organ.) J.* 18:6221–6227.

Di Cristina, M., R. Spaccapelo, D. Soldati, B. Bistoni, and A. Crisanti. 2000. Two conserved amino acid motifs mediate protein targeting to the micronemes of the apicomplexan parasite *Toxoplasma gondii*. *Mol. Cell. Biol.* 20: 7332–7341.

Donald, R.G., and D.S. Roos. 1998. Gene knock-outs and allelic replacements in *Toxoplasma gondii*: HXGPRT as a selectable marker for hit-and-run mutagenesis. *Mol. Biochem. Parasitol*. 91:295–305.

Donald, R.G.K., D. Carter, B. Ullman, and D.S. Roos. 1996. Insertional tagging, cloning, and expression of the *Toxoplasma gondii* hypoxanthine-xanthine-guanine phosphoribosyltransferase gene. Use as a selectable marker for stable transformation. *J. Biol. Chem*. 271:14010–14019.

Fourmaux, M.N., A. Achbarou, O. Mercereau-Puijalon, C. Biderre, I. Briche, A. Loyens, C. Odberg-Ferragut, D. Camus, and J.F. Dubremetz. 1996. The MIC1 microneme protein of *Toxoplasma gondii* contains a duplicated receptor-like domain and binds to host cell surface. *Mol. Biochem. Parasitol*. 83: 201–210.

Frand, A.R., J.W. Cuozzo, and C.A. Kaiser. 2000. Pathways for protein disulphide bond formation. *Trends Cell Biol*. 10:203–209.

Garcia-Réguet, N., M. Lebrun, M.-N. Fourmaux, O. Mercereau-Puijalon, T. Mann, C.J.M. Beckers, B. Samyn, J. Van Beeumen, D. Bout, and J.F. Dubremetz. 2001. The microneme protein MIC3 of *Toxoplasma gondii* is a secretory adhesin which binds to both the surface of the host cells and the surface of the parasite. *Mol. Microbiol.* In press.

Glombik, M.M., and H. Gerdes. 2000. Signal-mediated sorting of neuropeptides and prohormones: Secretory granule biogenesis revisited. *Biochimie*. 82:315–326.

Hager, K.M., B. Striepen, L.G. Tilney, and D.S. Roos. 1999. The nuclear envelope serves as an intermediary between the ER and Golgi complex in the intracellular parasite *Toxoplasma gondii*. *J. Cell Sci*. 112:2631–2638.

Hirst, J., and M.S. Robinson. 1998. Clathrin and adaptors. *Biochim. Biophys. Acta*. 1404:173–193.

Hoppe, H.C., H.M. Ngo, M. Yang, and K.A. Joiner. 2000. Targeting to rhoptry organelles of *Toxoplasma gondii* involves evolutionarily conserved mechanisms. *Nat. Cell Biol*. 2:449–456.

Kaasch, A.J., and K.A. Joiner. 2000. Protein-targeting determinants in the secretory pathway of apicomplexan parasites. *Curr. Opin. Microbiol.* 3:422–428.

Kappe, S., T. Bruderer, S. Gantt, H. Fujioka, V. Nussenzweig, and R. Menard. 1999. Conservation of a gliding motility and cell invasion machinery in apicomplexan parasites. *J. Cell Biol*. 147:937–944.

Karsten, V., H. Qi, C.J. Beckers, A. Reddy, J.F. Dubremetz, P. Webster, and K.A. Joiner. 1998. The protozoan parasite *Toxoplasma gondii* targets proteins to dense granules and the vacuolar space using both conserved and unusual mechanisms. *J. Cell Biol*. 141:1323–1333.

Kim, K., D. Soldati, and J.C. Boothroyd. 1993. Gene replacement in *Toxoplasma gondii* with chloramphenicol acetyltransferase as selectable marker. *Science*. 262:911–914.

Laemmli, U.K. 1970. Cleavage of structural protein during the assembly of the head of bacteriophageT4. *Nature*. 227:680–685.

Marks, M.S., H. Ohno, T. Kirchausen, and J.S. Bonifacino. 1997. Protein sorting by tyrosine-based signals: adapting to the Ysand wherefores. *Trends Cell Biol*. 7:124–128.

McMullen, B.A., K. Fujikawa, and E.W. Davie. 1991a. Location of the disulfide bonds in human coagulation factor XI: the presence of tandem apple domains. *Biochemistry*. 30:2056–2060.

McMullen, B.A., K. Fujikawa, and E.W. Davie. 1991b. Location of the disulfide bonds in human plasma prekallikrein: the presence of four novel apple domains in the amino-terminal portion of the molecule. *Biochemistry*. 30:2050–2056.

Morrissette, N.S., and D.S. Roos. 1998. *Toxoplasma gondii*: a family of apical antigens associated with the cytoskeleton. *Exp. Parasitol*. 89:296–303.

Naitza, S., F. Spano, K.J.H. Robson, and A. Crisanti. 1998. The trombospondin-related protein family of apicomplexan parasites: the gears of the cell invasion machinery. *Parasitol. Today*. 14:479–484.

Ngo, H.M., H.C. Hoppe, and K.A. Joiner. 2000. Differential sorting and post-secretory targeting of proteins in parasitic invasion. *Trends Cell Biol*. 10:67–72.

Sibley, L.D., S. Hakansson, and V.B. Carruthers. 1998. Gliding motility: an efficient mechanism for cell penetration. *Curr. Biol*. 8:R12–14.

Soldati, D., and J.C. Boothroyd. 1993. Transient transfection and expression in the obligate intracellular parasite *Toxoplasma gondii*. *Science*. 260:349–352.

Soldati, D., and J.C. Boothroyd. 1995. A selector of transcription initiation in the protozoan parasite *Toxoplasma gondii*. *Mol. Cell. Biol*. 15:87–93.

Sultan, A.A., V. Thathy, U. Frevert, K.J. Robson, A. Crisanti, V. Nussenzweig, R.S. Nussenzweig, and R. Menard. 1997. TRAP is necessary for gliding motility and infectivity of plasmodium sporozoites. *Cell*. 90:511–522.

Thiele, C., H.H. Gerdes, and W.B. Huttner. 1997. Protein secretion: puzzling receptors. *Curr. Biol*. 7:R496–500.

Tomley, F.M., and D. Soldati. 2001. Mix and match modules: structure and function of microneme proteins in apicomplexan parasites. *Parasitol. Today*. In press.

Wan, K.L., V.B. Carruthers, L.D. Sibley, and J.W. Ajioka. 1997. Molecular characterization of an expressed sequence tag locus of *Toxoplasma gondii* encoding the micronemal protein MIC2. *Mol. Biochem. Parasitol*. 84:203–214.

Yuda, M., H. Sakaida, and Y. Chinzei. 1999. Targeted disruption of the *Plasmodium berghei* CTRP gene reveals its essential role in malaria infection of the vector mosquito. *J. Exp. Med*. 190:1711–1716.